Rayyan *et al. BMC Oral Health* (2026) 26:1670
https://doi.org/10.1186/s12903-026-09357-5

BMC Oral Health

RESEARCH **Open Access**

Thermo-mechanical loading of innovative "Mini-skirt" preparation design versus conventional full-coverage maxillary central incisor preparation design: an in vitro study

Mohammad Rayyan[1], Rana Walid Tawil[2], Dana El Ballouli[3], Ehab A. Farghaly[4], Radwa Ibrahim Eltahawi[5], Mohamed B. A. Badawy[6], Omar Badran[7], Omayma Tantawy Said Mohammed[5], Alaa Mohamed Naguib[8], Nasser Hussein Shaheen[9], Mohamed Sayed[10*], Sahar Mokhtar[11], Mohammed Moustafa Shalaby[12], Hatem M. Ibrahim[13] and Maha Fouad[14]

Abstract

Background Conventional full-coverage anterior crown preparations for zirconia often require substantial enamel and dentine reduction and may concentrate palatal-cervical stresses, risking marginal discrepancy and compromised seal. A conservative "Mini-skirt" (MS) design that positions the palatal finish line coronally (above the cingulum) could preserve tooth structure and enhance adhesive support, but its thermo-mechanical performance under thermal cycling and fatigue loading remains unclear.

Purpose To evaluate whether a conservative MS anterior preparation, with a palatal finish line above the cingulum, improves the thermo-mechanical behavior of generation-5 zirconia crowns compared with a conventional full-coverage (CF) design.

Methods Sixty extracted maxillary central incisors were randomly assigned to MS or CF groups ($n = 30$). Monolithic 4Y zirconia crowns were CAD/CAM-manufactured, air-abraded and adhesively luted. Specimens were thermocycled 10,000 times between 5 °C and 55 °C, then obliquely loaded at 45° for 1.7×10^6 cycles (50 N, 2 Hz); survivors underwent static fracture testing (0.5 mm·min^{-1}). Marginal gaps were quantified from silicone replicas; failures were classified Grades I–IV (restorable = I–III). Finite-element models (~ 1.3 M elements) reproduced boundary conditions to map stress.

Results The MS preparation endured thermo-mechanical ageing markedly better than CF: 93.3% (28/30) versus 53.3% (16/30) of crowns completed the fatigue protocol ($\chi^2 = 9.01$, $p = 0.003$). Post-fatigue, median fracture load increased from 860 N (IQR 780–930 N) in CF to 1,140 N (1,030–1,260 N) in MS ($p < 0.05$). Mean marginal gap contracted from 112 ± 21 µm to 67 ± 14 µm (40% reduction, $p < 0.001$). Restorable fractures predominated in MS (83%) but were minority in CF (37%); catastrophic Grade IV failures fell from 63% to 17% ($\chi^2 = 13.6$, $p < 0.001$). Finite-element analysis

*Correspondence:
Mohamed Sayed
mohamed.elsayed@acu.edu.eg
Full list of author information is available at the end of the article

© The Author(s) 2026, modified publication 2026. **Open Access** This article is licensed under a Creative Commons Attribution-NonCommercial-NoDerivatives 4.0 International License, which permits any non-commercial use, sharing, distribution and reproduction in any medium or format, as long as you give appropriate credit to the original author(s) and the source, provide a link to the Creative Commons licence, and indicate if you modified the licensed material. You do not have permission under this licence to share adapted material derived from this article or parts of it. The images or other third party material in this article are included in the article's Creative Commons licence, unless indicated otherwise in a credit line to the material. If material is not included in the article's Creative Commons licence and your intended use is not permitted by statutory regulation or exceeds the permitted use, you will need to obtain permission directly from the copyright holder. To view a copy of this licence, visit http://creativecommons.org/licenses/by-nc-nd/4.0/.

corroborated the laboratory data, showing a 40% drop in peak palatal-cervical von Mises stress (415 to 250 MPa) and parallel reductions in tensile dentine stress and cement-shear hotspots.

Conclusions Within the limitations of this in vitro study, the MS preparation showed favorable biomechanical performance under simulated thermo-mechanical loading. These findings provide a preclinical rationale for further investigation of the MS design, although long-term clinical studies are required before definitive clinical recommendations can be made.

Keywords Conservative preparation, Failure mode, Finite-element analysis, Marginal adaptation, Thermo-mechanical fatigue, Zirconia crowns

Background

Restorative dentistry has always stood at the intersection of conservation and endurance, preserving as much healthy tissue as possible while ensuring that the restoration can survive decades of thermo-mechanical insult inside the mouth. Preparation geometry is the clinician's primary engineering control: it dictates the thickness and position of restorative material, the amount of supporting enamel and dentine retained, and the direction in which functional and thermal stresses are shunted through the crown–tooth complex [1, 2]. For maxillary central incisors the status-quo geometry since the 1980s has been a full-coverage preparation following the cervical margin [3]. Although this design reliably provides retention and allows space for modern ceramics, Finite-element analysis (FEA) and in vitro fatigue studies have revealed three persistent liabilities: (i) palatal cervical stress peaks that precipitate marginal micro-cracks (ii) unnecessary axial reduction that sacrifices valuable tooth structure, and (iii) sub-optimal bonding where the margin terminates on cementum rather than enamel [4, 5].

In search of a geometry that mitigates these shortcomings without compromising aesthetics, the Mini-skirt (MS) preparation was proposed. The defining feature is a palatal finish line raised around 0.5 mm above the cingulum, coupled with a modest 0.4 mm axial reduction that preserves more coronal tissue. By relocating the margin into the thicker enamel of the palatal zone, the design aims to: (a) spare more valuable tooth structure [4], (b) finish the palatal margin in enamel and dentine for better bonding [6], and (c) simplify margin visualization for both clinician and technician [7, 8].

The convergence of digital dentistry and high-strength polycrystalline ceramics amplifies the MS design's clinical appeal. CAD/CAM milling allows micron-level reproduction of the elevated palatal finish line, while contemporary adhesive systems provide durable bonds even on minimal enamel widths [9, 10].

Teeth endure approximately 2,300 chewing cycles·day^{-1} and experience abrupt thermal excursions whenever a patient alternates hot coffee with cold water [11]. This thermo-mechanical loading produces cyclic tensile/compressive strains and repeated thermal-shock events that challenge both the restorative material and the adhesive luting layer. A preparation that merely survives static load testing is therefore no guarantee of long-term success [12, 13].

Potential clinical and sustainability implications remain speculative and require confirmation through future clinical and life-cycle studies. Finite-element analysis (FEA) was included as a complementary computational method to support the mechanical findings by identifying stress-distribution patterns within the crown–tooth complex. In the present study, FEA was used to examine whether differences in fatigue survival, fracture resistance, marginal integrity, and failure mode could be explained by changes in palatal-cervical stress concentration and interfacial load transfer [14].

The present study hypothesizes that the MS geometry will outperform the conventional design in: fracture resistance and fatigue survival, marginal integrity, and overall failure-mode distribution favoring restorable type of failures.

A secondary aim is to triangulate mechanical findings with FEA-derived stress maps so that any performance differences can be mechanistically explained. By delivering an integrated mechanical-computational assessment, this work seeks to clarify whether the theoretical advantages of the MS preparation are supported by controlled laboratory and computational findings.

Methods

Study setting

The investigation was conducted over seven months in 2025 in the CAD/CAM Unit, Prosthodontics Department, Faculty of Oral and Dental Medicine, Nahda University, Beni Suef, Egypt. The protocol received approval from the Institutional Review Board of the Faculty of Oral and Dental Medicine, Nahda University (IRB #003-9-25-3). Extracted maxillary central incisors obtained during periodontal surgeries with informed patient consent were used, and each sample was coded to safeguard donor anonymity. All procedures conformed to the Declaration of Helsinki and to applicable national and institutional guidelines governing the ethical use of human tissues [15].

Study design

A controlled in vitro experimental design was adopted to compare two maxillary-central-incisor preparation geometries under simulated oral conditions.

Sample size calculation

The primary endpoint of this study was thermo-mechanical fatigue survival, defined as the proportion of specimens completing the aging/fatigue protocol without catastrophic failure. Therefore, the a priori sample-size calculation was performed using G*Power software (Version 3.1, Heinrich-Heine-Universität Düsseldorf, Düsseldorf, Germany) for a two-sided comparison of two independent proportions. The calculation was based on an α level of 0.05, statistical power of 80%, and an allocation ratio of 1:1. The expected survival proportions were estimated as 90% for the Mini-skirt (MS) group and 60% for the conventional full-coverage (CF) group, based on preliminary pilot/manufacturer data, corresponding to an assumed effect size of Cohen's h = 0.73. The minimum required sample size was 30 specimens per group. Accordingly, a total of 60 extracted maxillary central incisors were included and equally allocated to the two study groups.

Teeth collection and preparation

Sixty freshly extracted maxillary central incisors having closely matched in labio-palatal and mesio-distal dimensions, were collected from the Department of Periodontology, Faculty of Oral and Dental Medicine, Nahda University. Teeth were discarded if they exhibited axial caries, unusually large or small restorations, crown or root fractures, or surface decalcification [16]. Dimensions were verified with a digital caliper, after which the teeth were stratified by crown morphology and randomly allocated into two groups of N = 30. Soft-tissue remnants and calculus were removed using ultrasonic scaler, and all specimens were sterilized in an autoclave at 121 °C (≈ 15 psi) for 20 min [17, 18].

Previous evidence suggests that steam autoclave sterilization may not necessarily alter dentine substrate behavior, as Pashley et al. reported no significant effect on dentine permeability or shear bond strength after sterilization of human teeth under their study conditions [19].

Teeth reduction and preservation

All preparations were performed by a single experienced operator (M.R.) under a dental operating microscope at ×10 magnification (ZEISS EXTARO 300, Carl Zeiss Meditec AG, Jena, Germany) to minimize operator variability. Before the main experiment, the operator was calibrated on pilot specimens using the same preparation protocol, burs, and reduction targets planned for the study. Calibration was considered acceptable only after repeated preparations showed consistent finish-line position, axial reduction, and incisal reduction within predefined tolerances. During specimen preparation, all teeth were mounted in a dental surveyor to standardize the path of insertion and overall convergence, and depth-orientation grooves were used to guide reduction. Reduction depth and finish-line location were checked at each step using a digital caliper and silicone index.

To provide independent verification, all prepared teeth were digitally scanned after preparation, and the scans were assessed against the planned preparation dimensions using CAD software. Margin position, axial reduction, and incisal reduction were measured at predefined reference points by an independent examiner. This workflow ensured both operator standardization and objective confirmation of preparation accuracy.

All tooth preparations were performed using a high-speed rotary handpiece under copious water cooling. Bulk tooth reduction was performed using round end taper (RET) carbide bur # H856U.314.016 ((Komet Dental/Gebr. Brasseler GmbH & Co. KG, Lemgo, Germany), whereas finish-line refinement and smoothing of the internal line angles were completed using carbide bur # H 856 U RET (Komet Dental/Gebr. Brasseler GmbH & Co. KG, Lemgo, Germany). The same bur sequence and instrumentation protocol were used for all specimens to ensure standardization of the preparations.

Mini-skirt preparation design

The MS preparation was performed as a conservative anterior full crown design in which the palatal finish line was raised coronally (~ 0.5 mm above the cingulum). On the palatal cervical third, axial reduction was limited to ~ 0.4 mm, and the palatal finish line in this region was prepared as a light chamfer margin matching the reduced thickness. The remaining surfaces followed standardized zirconia crown reduction targets: incisal reduction 2.0 mm (two-plane), labial reduction 1.0 mm (three-plane), and proximal reduction 0.8 mm, all with rounded internal line angles. A continuous circumferential finish line was maintained, with the facial/proximal margin prepared as a deep chamfer of 0.4–1.0 mm, while the palatal margin transitioned smoothly into the coronally displaced MS without sharp steps. Total occlusal convergence was standardized to approximately 6°, and a uniform insertion path was maintained (Figures 1, 2 and 3).

Conventional full-coverage preparation design

The CF preparation was executed as a traditional circumferential anterior crown preparation with the finish line following the cervical contour around the entire tooth, including the palatal aspect (no coronal displacement). Reduction targets were standardized as follows: incisal reduction 2.0 mm (two-plane), labial reduction 1.0 mm

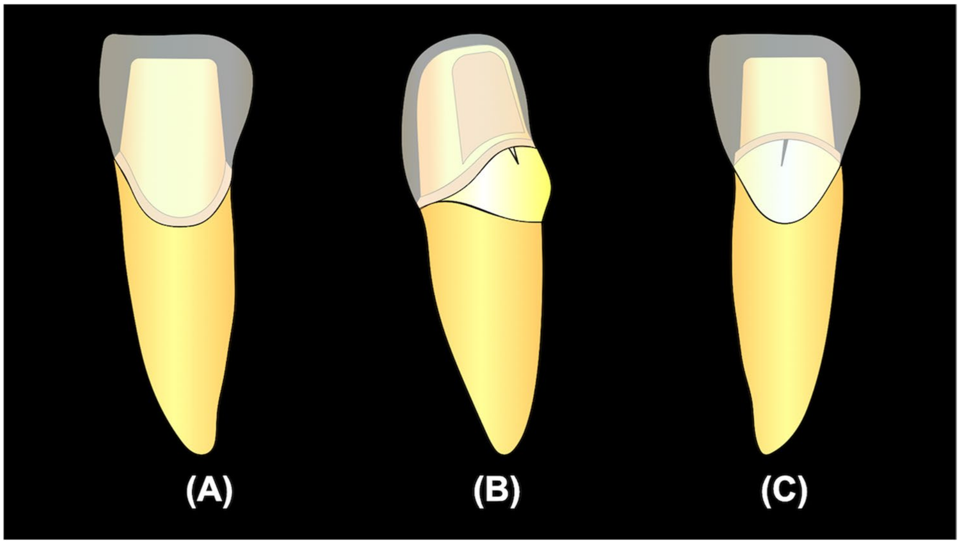

Fig. 1 Diagram of MS preparation design

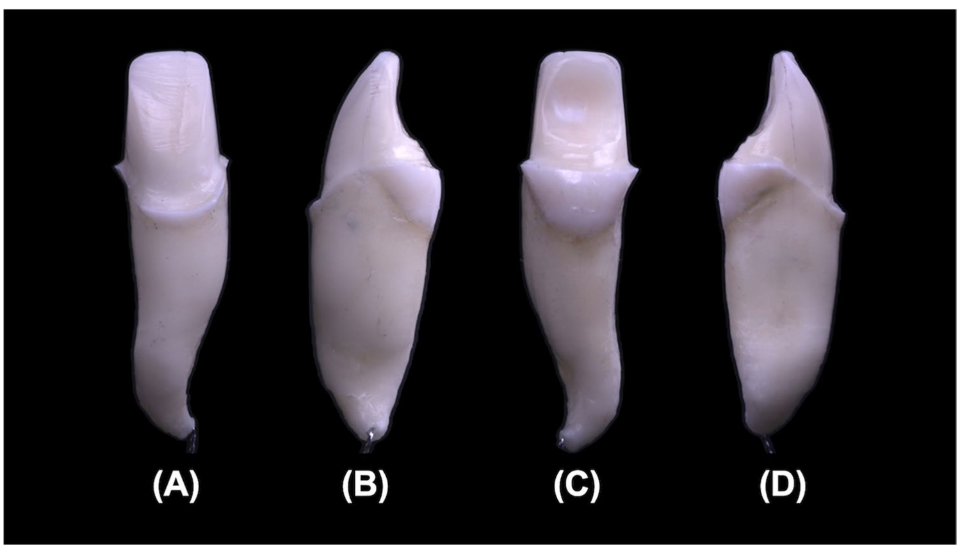

Fig. 2 Conservative MS maxillary central incisor preparation with the palatal finish line raised above the cingulum and reduced axial reduction

(three-plane), palatal axial reduction 0.4 mm, and proximal reduction 0.8 mm, with all internal angles rounded. The circumferential finish line was prepared as a deep chamfer of ~0.4–1.0 mm to support monolithic zirconia thickness requirements and seating accuracy. Total occlusal convergence was maintained at approximately 6°, with a continuous, clearly defined margin and smooth transitions to minimize localized stress concentration. (Fig. 4)

Following preparation, the specimens were immersed in sterile 0.9% saline to prevent desiccation. Before experimentation, each tooth was screened under a stereomicroscope (2.5×) to ensure it was free of cracks or other defects [20].

Pseudo periodontal ligament addition

A 0.2 mm coat of molten wax was painted onto each root stopping 1 mm apical to the cementoenamel junction (CEJ) to simulate the periodontal ligament. Using a paralleling jig, the teeth were set upright in self-curing acrylic cylinders (Axcent Orthodontic Acrylic, Garreco LLC, Heber Springs, AR, USA; 20 mm diameter × 25 mm height). After the resin cured, the teeth were removed and all wax was peeled from both the roots and the acrylic sockets. Light-body polyvinyl siloxane (PVS) (Virtual Light Body, Ivoclar Vivadent AG, Schaan, Liechtenstein) was then injected into the space between each tooth and its socket, and any material rising above the CEJ was trimmed away with a No. 12 surgical blade [21] (Figures 5, 6 and 7).

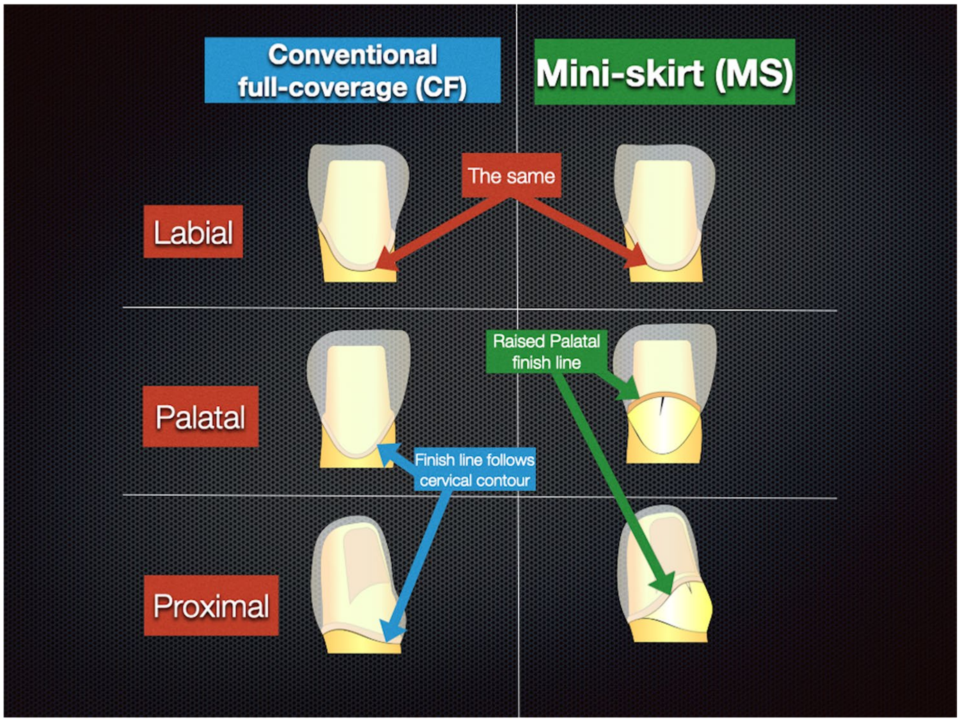

Fig. 3 Schematic comparison of conventional full-coverage (CF) and Mini-skirt (MS) preparation designs in labial, palatal, and proximal views, highlighting the coronally raised palatal finish line in the MS design

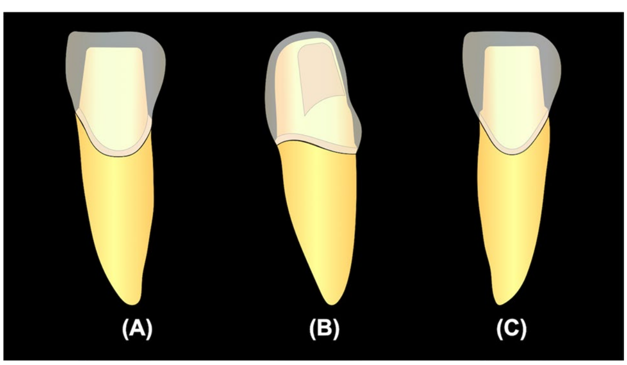

Fig. 4 Diagram of CF preparation design

Specimens grouping

The 60 specimens were stratified by preparation type and randomly assigned to two equal groups ($N = 30$): Group MS, receiving the Mini-skirt preparation, and Group CF, receiving the conventional full-coverage preparation.

Zirconia crown fabrication

All dies were scanned individually with an intraoral digital scanner (Medit i700, Medit Corp., Seoul, Republic of Korea). For each preparation design, a single monolithic zirconia crown replicating a maxillary central incisor was digitally designed. Generation-5 monolithic zirconia blocks (Art, White Stone Advanced Dental Materials, Cairo, Egypt) were then dry-milled on a five-axis milling unit (ED5X, EMAR, 10th of Ramadan City, Sharqia, Egypt). The milled crowns were collected, inspected, and sintered following the manufacturer's prescribed firing schedule. Final finishing and high-gloss polishing were performed with dedicated rubber discs (ZiLMaster Finishing & Polishing Kit HP, Shofu Inc., Kyoto, Japan). (Figures 8, 9, 10 and 11)

Zirconia crown cementation

Each crown was first trial-seated on its corresponding resin die. Dentine surfaces were conditioned with 39% phosphoric acid gel (TOKUYAMA® ETCHING GEL HV, Tokuyama Dental Corporation, Tokyo, Japan) for 5 s, then rinsed for 20 s. A universal adhesive (PALFIQUE BOND, Tokuyama Dental Corporation, Tokyo, Japan) was applied for 10 s, gently air-thinned for 10 s, and light-cured for 10 s. The crown interiors were air-abraded with 50 µm aluminum-oxide particles, cleaned with alcohol, and dried with oil-free air. A ceramic primer (TOKUYAMA UNIVERSAL PRIMER, Tokuyama Dental Corporation, Tokyo, Japan) was applied and air-dried for 5 s. Adhesive resin cement (ESTECEM Plus, Tokuyama Dental Corporation, Tokyo, Japan) was injected into each crown, which was then seated on its tooth under a constant 5 kg load for 10 min; excess cement was cleared after 3–5 min. Final polymerization was performed using an LED light-curing unit with an output intensity of approximately 1200 mW/cm² and a wavelength range of about 430–480 nm. The light tip was positioned as close

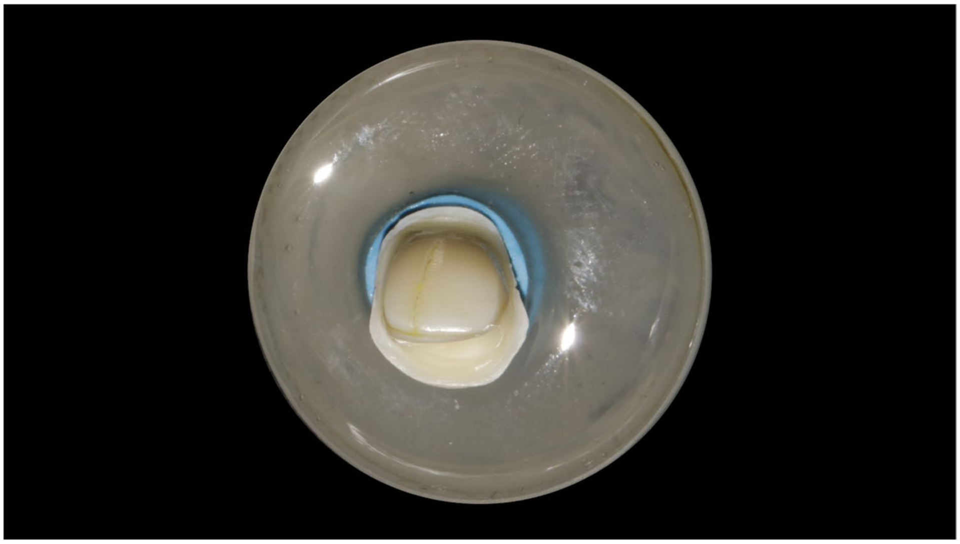

Fig. 5 Simulation of the periodontal ligament: teeth embedded in acrylic blocks with a 0.2-mm polyvinyl siloxane layer around the roots

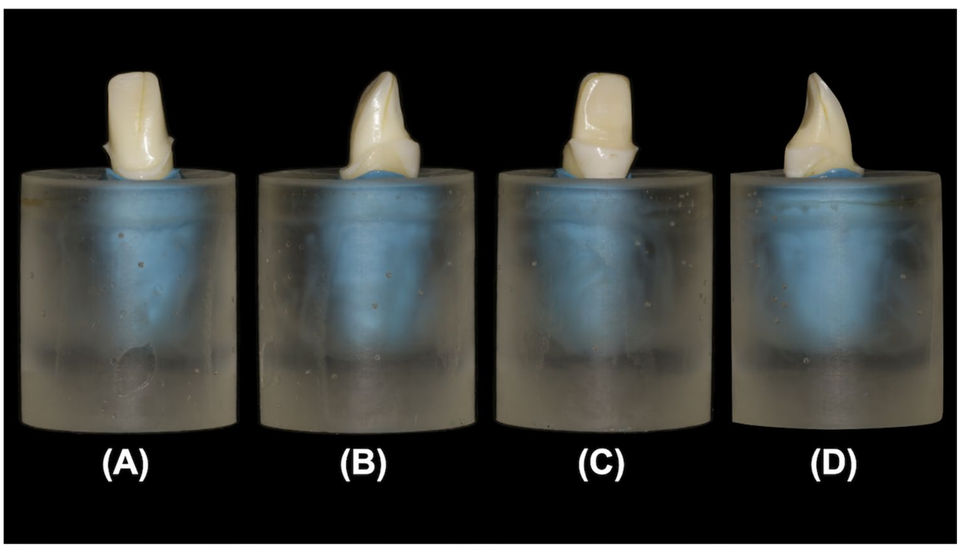

Fig. 6 Conservative MS maxillary central incisor placed in epoxy resin block with PDL simulation

as possible to the crown surface during curing, and each surface was light-cured for 40 s according to the standardized cementation protocol [15, 22] (Fig. 12).

Thermal cycling of specimens

Each specimen underwent 10,000 thermal cycles in a thermocycler (THE-1200, SD Mechatronik GmbH, Feldkirchen-Westerham, Germany), alternating 30 s at 5 °C and 20 s at 55 °C, with a 10-s transfer interval between baths.

Marginal-integrity evaluation with the addition-silicone replica technique

Light-body PVS (Virtual Light Body, Ivoclar Vivadent AG, Schaan, Liechtenstein) was syringed into the crown cavity, avoiding air entrapment. Each crown was seated on its corresponding tooth and loaded vertically to 50 N for the manufacturer's recommended setting time plus 1 min (total ≈ 5 min) to ensure complete polymerization. Without disturbing the assembly, heavy-body PVS (Virtual Heavy Body, Ivoclar Vivadent AG, Schaan, Liechtenstein) was injected to fill the entire crown and circumferentially around the margin; the material was allowed to set (≈ 3 min). The crown–replica complex was then removed en bloc. The resulting replica consisted of a light-body liner, an internal heavy-body core filling the crown, and an external heavy-body base at the margin. Each replica was sectioned buccopalatal and mesiodistal with a No. 11 surgical blade (hand-driven). Calibrated images were captured under a stereomicroscope (20×).

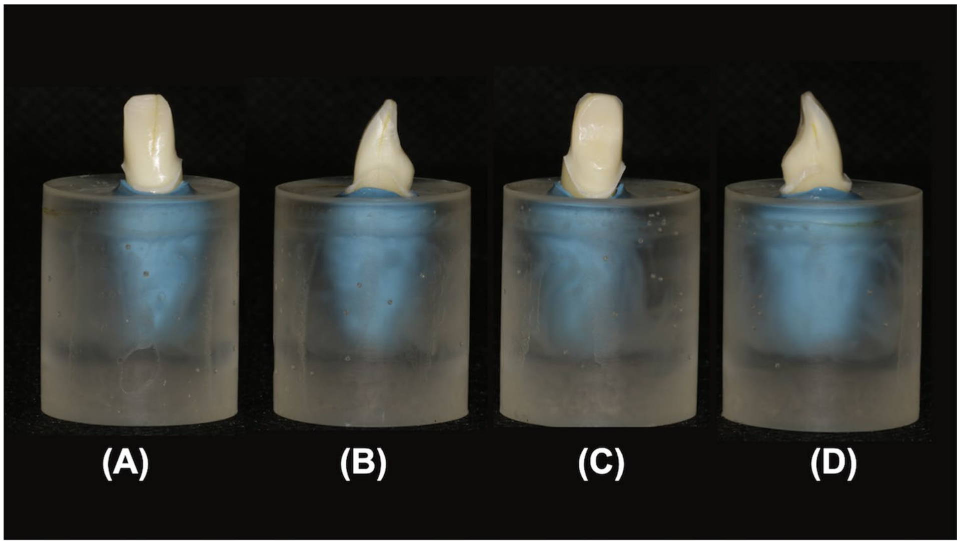

Fig. 7 CF maxillary central incisor placed in epoxy resin block with PDL simulation

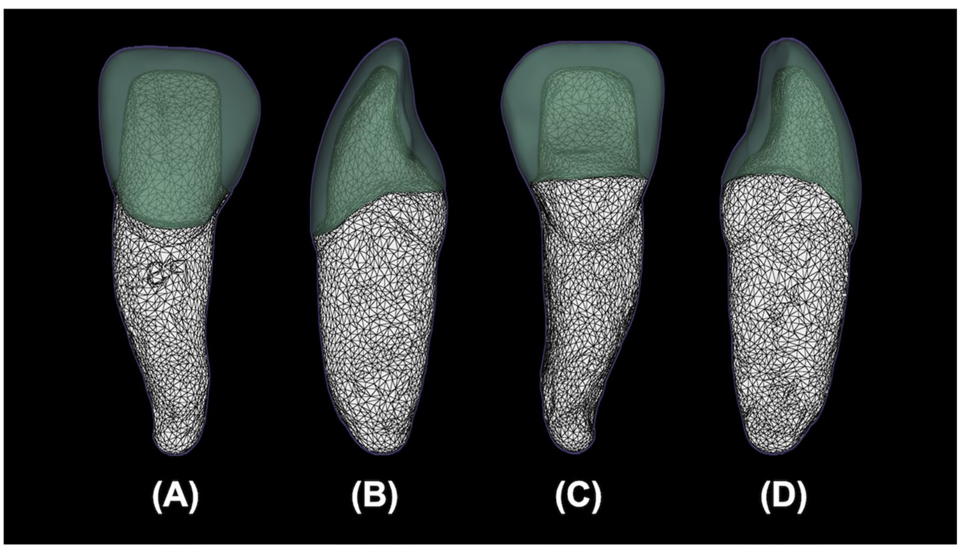

Fig. 8 Digital impressions and CAD design of monolithic zirconia crowns on standardized MS preparation

Light-body PVS film thickness was measured at the labial, palatal, mesial, and distal margins at 10 evenly spaced points per margin. For reliability, a second blinded examiner re-measured 20% of the sections.

Fatigue-testing protocol

The fatigue protocol was chosen to simulate functional loading of maxillary anterior teeth. The load was applied at 45° to the long axis to reproduce the oblique palatal contact pattern associated with incisal guidance and protrusive function, thereby generating clinically relevant tensile and shear stresses in the palatal cervical region [23–26].

A digital inclinometer verified ± 0.3°. Tests were performed on an electrodynamic universal testing machine (ElectroPuls E3000, Instron, Norwood, MA, USA) with a 3 kN load cell (± 0.5% FS) and an LVDT displacement transducer (± 0.1 mm). A polished stainless-steel hemispherical indenter (4 mm radius) was mounted at the same 45° inclination and aligned to the mid-palatal fossa. The indenter was replaced after every ten specimens to avoid surface roughening [27].

Sinusoidal force-control loading was used: 5–50 N (R = 0.1) at 2 Hz (120 cycles·min^{-1}), which completes approximately 1.7 × 10^6 cycles in approximately 10 days while limiting self-heating of the zirconia core. Before cycling, a 10 N seating load was applied for 60 s to stabilize the crown–cement–tooth complex and vent trapped air from the water chamber. Each specimen was run for 1.7 × 10^6 cycles, corresponding to approximately 2 clinical years,

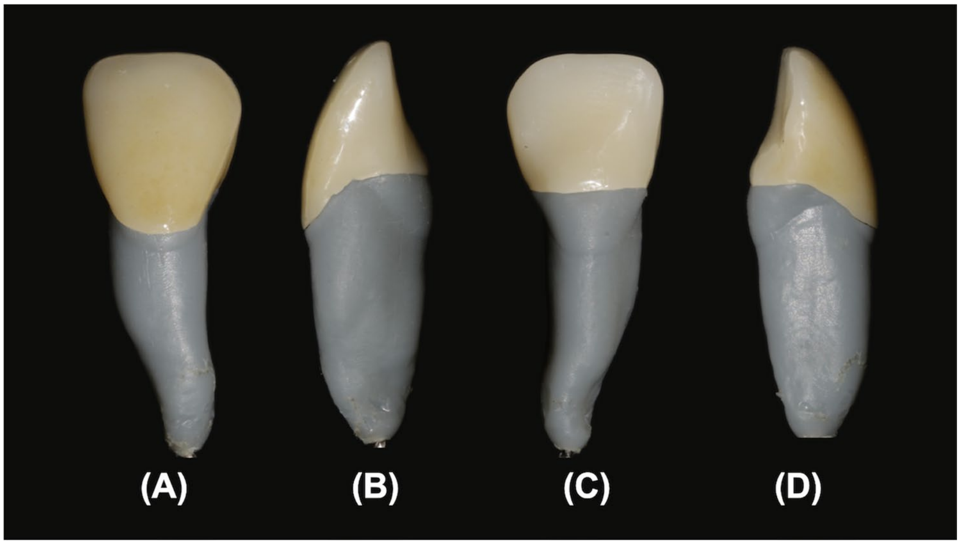

Fig. 9 MS monolithic zirconia crown on 3D printed resin die

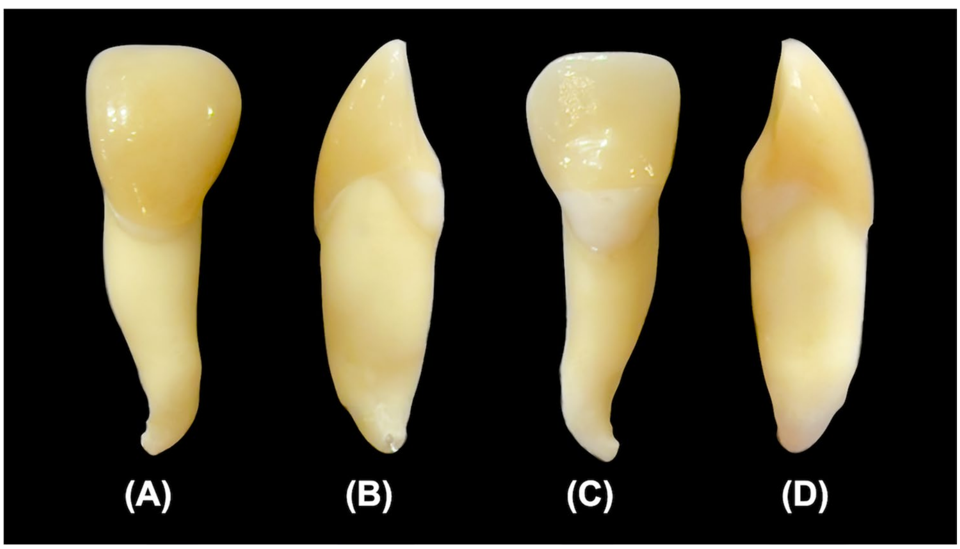

Fig. 10 MS Monolithic zirconia crown on standardized MS preparation

assuming approximately 2,300 cycles·day^{-1} [9]. Specimens completing the schedule were classified as run-outs.

Failure was automatically flagged by either: (i) A sudden 10% drop in peak load for three consecutive cycles (typical of crack-through or cement rupture), (ii) excess displacement (>0.05 mm beyond the elastic range), (iii) manual termination when an audible crack or visible dislodgement was detected through the transparent chamber wall. Immediately after cycling, the crown was loaded to catastrophic fracture at a cross-head speed of 0.5 mm·min^{-1}. (ISO 6872 compliant). Peak fracture load (N) and energy-to-fracture (area under the load–displacement curve) were recorded.

Failure mode and restorability index

Following fracture-testing, each specimen was examined by three operators, both unaided and with a 3.5 × surgical loupe (Lupa, Bio-Art Equipamentos Odontológicos Ltda., São Carlos, SP, Brazil). Failures were classified according to a modified restorability scheme :

- Grade I – fracture confined to the crown.
- Grade II – fracture limited to the tooth, within the coronal third of the root.
- Grade III – fracture involving both crown and tooth, within the coronal third of the root.
- Grade IV – tooth fracture (with or without crown involvement) extending beyond the coronal third of the root.

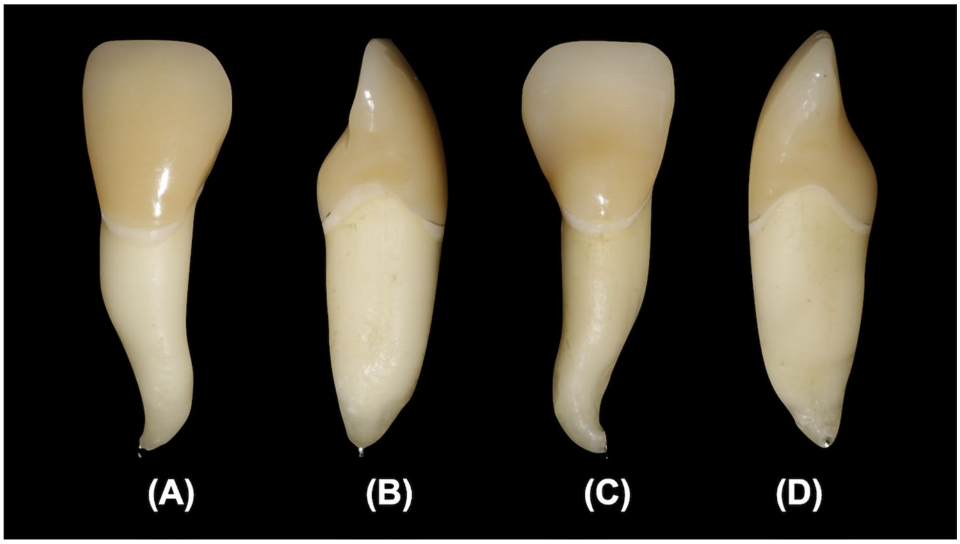

Fig. 11 Monolithic zirconia crown on standardized CF preparation

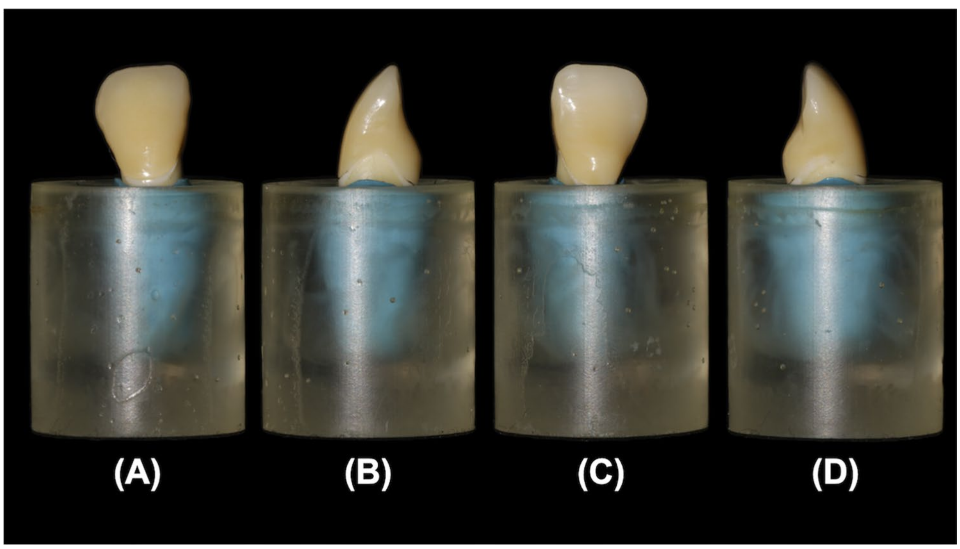

Fig. 12 Cemented zirconia crowns to the corresponding teeth: CF specimen

Grades I–III were deemed restorable, whereas Grade IV was considered non-restorable (Fig. 13).

Finite-element analysis (FEA)

STL files of both crown and tooth were exported into Mimics 25.0 (Materialise NV, Leuven, Belgium). Enamel, dentine, resin cement, zirconia crown, periodontal-ligament (PDL) layer (0.2 mm), and acrylic embedding block were segmented as separate volumes. Stair-step artifacts were smoothed in 3-Matic 17.0, sharp edges at the finish lines were retained to preserve geometric fidelity. The six solids were exported to ANSYS Workbench 2024 R2 (ANSYS, Inc., Canonsburg, PA, USA) for meshing and analysis. The FEA model was verified through geometric verification, mesh-convergence testing, and matching of the computational boundary conditions to the experimental setup. The segmented models were visually inspected to confirm preservation of the finish-line geometry, crown margins, cement layer, periodontal-ligament simulation, and acrylic embedding block. Mesh convergence was confirmed when further mesh refinement changed the peak von Mises stress by less than 5%.

All materials were defined as homogeneous, isotropic and linearly elastic (Table 1). These assumptions were adopted to simplify the computational model and allow direct comparison between the two preparation designs under identical boundary conditions. The elastic moduli were selected from published dental FEA literature and manufacturer-provided material data to represent commonly accepted mechanical parameters

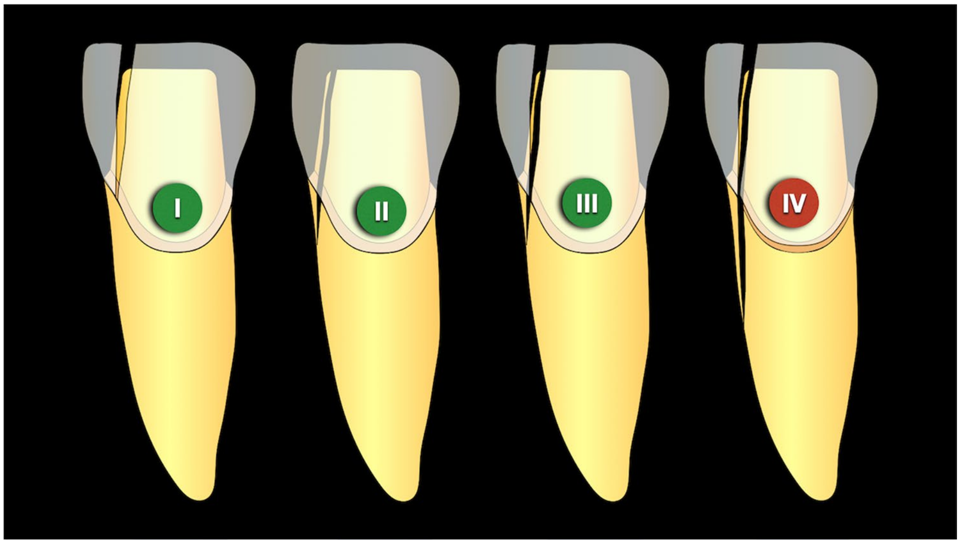

Fig. 13 Modified failure-mode and restorability scheme (Grades I–IV) used to classify crown and root fractures. Grade I to III restorable, while grade IV irrestorable

Table 1 Elastic moduli of model components

Component	Elastic modulus (GPa)
Zirconia crown	210
Resin cement	8.7
Enamel	84
Dentine	18.6
Periodontal ligament	0.068
PMMA acrylic block	2.7

for enamel, dentine, zirconia, resin cement, periodontal ligament simulation, and acrylic embedding material. Elastic moduli for dental tissues were taken from validated meta-analyses; zirconia and cement values were manufacturer-supplied. Poisson's ratio for all materials was 0.30 ± 0.02.

All adjoining solids were set as perfectly bonded to emulate complete adhesive coverage. The basal surface of the acrylic cylinder was fixed in all translational and rotational degrees of freedom. A static 250 N force, oriented 45° to the long axis, was applied over a 1 mm-diameter patch on the palatal fossa (matching the experimental loading indent). Peak von Mises and maximum principal stresses in crown, cement and dentine, contact pressure along the finish line, and total displacement of the crown tip (deformation) were evaluated.

Statistical analysis

All statistical computations were performed with IBM SPSS Statistics v28 (IBM SPSS Statistics v28, IBM Corp., Armonk, NY, USA). Descriptive statistics was done for each continuous variable (e.g., fracture resistance), the mean ± standard deviation (SD) was reported when data followed a normal distribution; otherwise the median and inter-quartile range (IQR) were provided. Failure mode (grades I–IV) were summarized as absolute counts and percentages. Normality of each continuous dataset was assessed with the Shapiro–Wilk test ($\alpha = 0.05$) and inspection of Q-Q plots. When the data met normality assumption, parametric tests were applied (Independent-samples *t*-test). If normality were violated, the corresponding non-parametric alternatives were used (Mann–Whitney *U* test). Associations between preparation design and categorical failure modes were examined with the χ^2 test of independence. The hazard ratio was calculated from the time-to-event (cycles-to-failure) data obtained during the thermo-mechanical fatigue test. For each specimen, the event variable was defined as fatigue failure during cyclic loading, and the time variable was the number of cycles completed before failure. Specimens that survived the full 1.7×10^6 cycles were considered censored observations.

Survival was analyzed using Kaplan–Meier curves and compared between groups using the log-rank test. The hazard ratio was estimated using a univariable Cox proportional hazards regression model, with preparation design as the predictor variable. The proportional hazards assumption was assessed by inspection of log-minus-log survival plots. No relevant violation of the proportional hazards assumption was detected. *P*-value < 0.05 was considered statistically significant.

Results

Thermo-mechanical fatigue survival

Under the combined regimen of 10,000 thermal exchanges (5 °C ↔ 55 °C) followed by 1.7×10^6 oblique load cycles (50 N, 2 Hz), 28 of 30 MS specimens and 16 of 30 CF specimens reached the preset "run-out" target (93.3% vs. 53.3%) (Table 2).

Table 2 Thermo-mechanical survival "run-out" by group

Group	Survived "run-out"	Survival rate
Mini-skirt (MS)	28 / 30	93.3%
Full-coverage (CF)	16 / 30	53.3%
Between-group (log-rank)	—	$\chi^2 = 9.01$ $p = 0.003$

Table 3 Post-fatigue fracture resistance by group

Statistic	MS	CF	Test
Median (IQR), N	1140 (1030–1260)	860 (780–930)	Mann–Whitney $U = 238$, $p = 0.012$
Mean ± SD, N	1137 ± 142	855 ± 128	Cohen's $d = 2.14$

Energy-to-fracture followed the same trend (MS = 18.4 ± 3.9 J vs. CF = 11.7 ± 2.8 J, $p < 0.001$)

Table 4 Marginal film thickness by margin location (mean ± SD, µm)

Margin	MS (mean ± SD)	CF (mean ± SD)	Δ (%)
Labial	69 ± 13	115 ± 22	–40%
Palatal	64 ± 15	118 ± 19	–46%
Mesial	66 ± 14	109 ± 20	–39%
Distal	70 ± 16	106 ± 23	–34%
Pooled	67 ± 14	112 ± 21	–40%

Two-way ANOVA: significant effects for both preparation design ($p < 0.001$) and margin location ($p = 0.032$) with no interaction ($p = 0.41$)

- Absolute risk of catastrophic failure: 6.7% (MS) vs. 46.7% (CF).
- Risk ratio (RR) for failure = 7.0 (95% CI 1.7–28.2), indicating that CF crowns were seven times more likely to fracture before the end of the cycling protocol.
- Kaplan–Meier analysis showed the steepest drop for CF between 0.6×10^6 and 1.1×10^6 cycles, whereas the two MS failures occurred late ($\geq 1.35 \times 10^6$ cycles), yielding a significant log-rank difference (χ^2 = 9.01, $p = 0.003$).
- A univariable Cox proportional hazards model showed a higher fatigue-failure hazard for the CF group compared with the MS group (hazard ratio = 2.9, 95% CI 1.4–6.1), indicating an almost three-fold higher probability of earlier failure for CF.

Static fracture resistance (post-fatigue)

Median fracture loads rose from 860 N (IQR 780–930 N) in CF to 1,140 N (IQR 1,030–1,260 N) in MS (*Mann-Whitney U* = 238, $p = 0.012$) (Table 3).

- Relative gain: +32% in favor of MS.
- The rank-biserial correlation ($r = 0.72$) reflects a large, practice-relevant effect.
- Assuming a clinical incisal occlusal force envelope of 150–300 N, both designs remained within an 8.0 safety factor for static overload, but the MS design retained a ≥ 30% residual reserve after aging, whereas CF often fell below a 3 × margin.

Marginal integrity (silicone-replica film thickness, µm)

Average replica-film thickness fell from 112 ± 21 µm (CF) to 67 ± 14 µm (MS), a 40% contraction that keeps MS comfortably below the widely accepted 120 µm clinical limit (Table 4) (Fig. 14).

- Coefficient of variation remained similar (MS 21%, CF 19%), suggesting the improvement was systematic rather than operator-dependent.

Failure-mode distribution and restorability

Using the modified four-grade scheme (I–IV), 25 of 30 MS specimens (83%) failed in restorable patterns (Grades I–III) versus only 11 of 30 CF crowns (37%), χ^2 = 13.6, $p < 0.001$ (Table 5) (Figs. 15 and 16).

- Most frequent MS failure: chipping confined to the crown body (Grade I) (Fig. 17).
- Most frequent MS failure: chipping confined to the crown body (Grade I) (Fig. 18).
- Between-group Restorability: RR = 2.27 (95% CI 1.38–3.74). Non-restorable risk reduction: dropped from 63% (CF) to 17% (MS), giving an ARR = 46% and NNT ≈ 2.2.

Finite-element analysis (FEA)

Digital twins reproduced the loading boundary conditions; peak von Mises stress at the palatal cervical region dropped from 415 MPa (CF) to 250 MPa (– 40%) in MS, with a broader, more coronal load-sharing footprint. Mesh-convergence testing confirmed numerical stability,

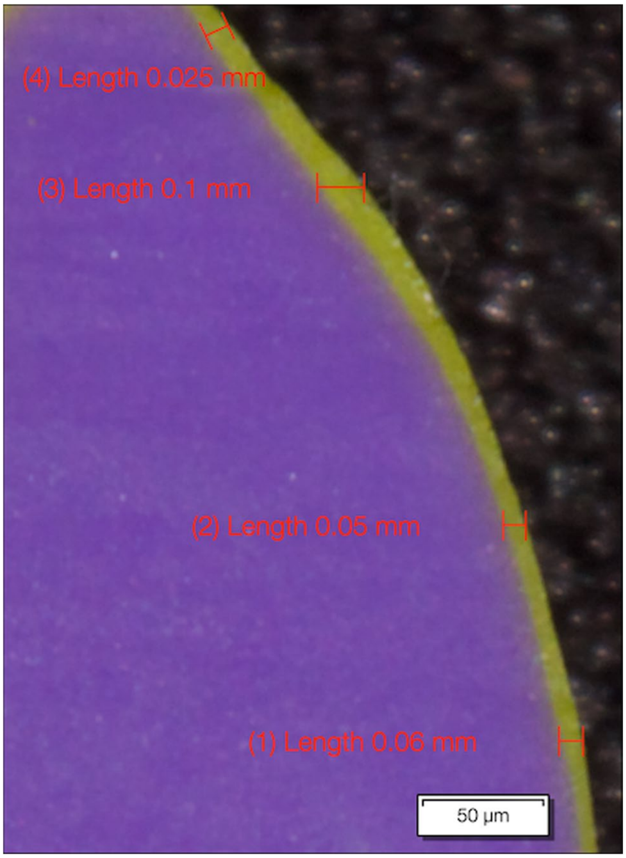

Fig. 14 Silicone replica technique: light-body and heavy-body polyvinyl siloxane layers used to reproduce the crown–tooth interface for marginal gap analysis

as further mesh refinement changed the peak von Mises stress by less than 5% (Table 6).

- Tensile stress in underlying dentine fell by 42%,
- Cement interfacial shear nodes > 25 MPa shrank from 29% to 12%.
- Tip displacement (250 N): 11.8 → 9.1 µm (– 23%), indicating a stiffer, better-integrated assembly.

Stress maps revealed a broader, coronally shifted load-sharing footprint in the MS geometry, corroborating the empirical improvements (Figs. 19, 20, 21 and 22).

A quantitative trend-based comparison between the FEA and laboratory outcomes showed concordant findings. The MS design reduced peak palatal-cervical von Mises stress by 40% compared with CF, which paralleled the 32% increase in post-fatigue fracture resistance, the 40% reduction in marginal gap values, and the lower proportion of catastrophic failures observed experimentally. Although this does not represent direct point-by-point validation of the computational model, it supports the mechanical consistency between the stress-distribution pattern and the experimental performance outcomes.

Integrated performance profile

Across endpoints, MS outperformed CF: higher fatigue survival (28/30 vs. 16/30; log-rank $\chi^2(1) = 9.01$, $P = 0.003$), lower failure risk (RR = 0.14, 95% CI [0.04, 0.58]), greater post-fatigue fracture resistance (median 1,140 vs. 860 N; U = 238, $P = 0.012$), smaller marginal gaps (67 ± 14 vs. 112 ± 21 µm; design effect $P < 0.001$), more restorable failures (83% vs. 37%; $\chi^2(1) = 13.6$, $P < 0.001$), and lower FEA stresses (250 vs. 415 MPa) (Table 7).

Discussion

The experimental design of the present investigation was intentionally layered to isolate the mechanical and biological consequences of a minimally invasive "Mini-skirt" preparation while maintaining strict parity in all other variables. The decision to bond monolithic generation-5 (4-Y) zirconia restorations to both preparation designs eliminated the veneer chipping seen in earlier bilayer systems and allowed the study to focus on structural failures originating at the crown–tooth interface rather than within a veneering ceramic [22, 28, 29].

The MS preparation demonstrated a more favorable mechanical response than the conventional full-coverage design after thermo-mechanical aging. Rather than simply delaying failure, the conservative geometry appeared to modify the pattern of stress transfer within the crown–tooth complex, resulting in improved fatigue behavior, greater residual strength, tighter marginal adaptation, and a shift toward more restorable fracture patterns.

Finite-element analysis provided a mechanistic explanation for these observations. Elevating the palatal finish line coronal to the cingulum appeared to broaden

Table 5 Failure modes by group

Failure grade	Mini-skirt (MS)	Full-coverage (CF)	χ^2 adjusted residual†
I	14 (46.7%)	6 (20.0%)	+ 2.1
II	8 (26.7%)	3 (10.0%)	+ 1.2
III	3 (10.0%)	2 (6.7%)	+ 0.3
Restorable (I–III)	25 (83.3%)	11 (36.7%)	
IV	5 (16.7%)	19 (63.3%)	–3.6

✧ Grades I–IV per the modified restorability scheme in the protocol. † Positive residuals indicate over-representation in MS; negative values indicate over-representation in CF

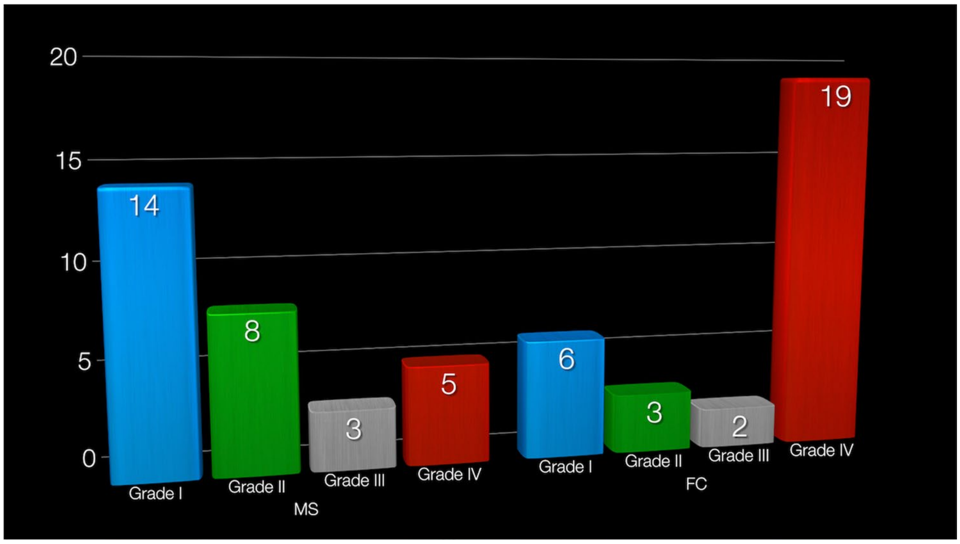

Fig. 15 Bar chart showing mode of failure in each group

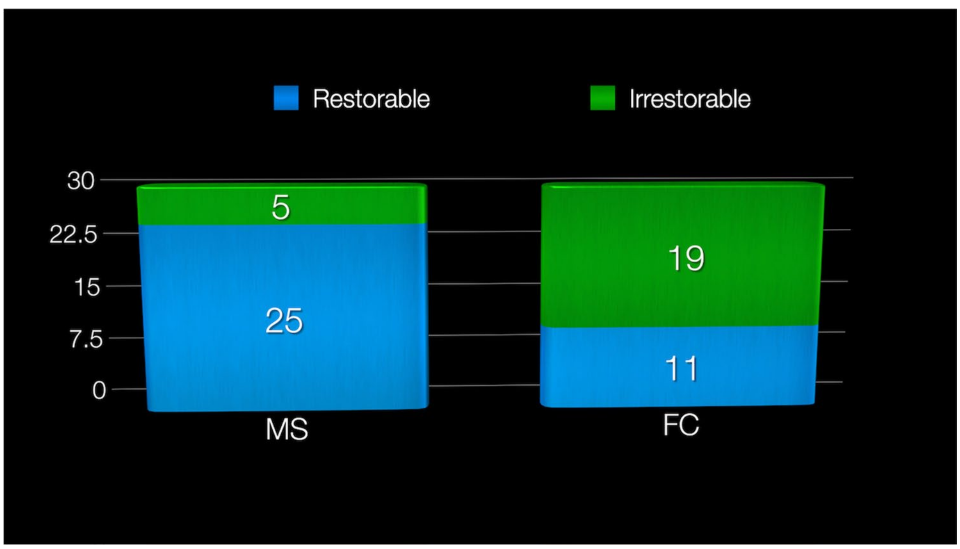

Fig. 16 Bar chart showing number of restorable fractures in each group

the load-bearing area and shift stress away from the vulnerable palatal-cervical region. This supports the interpretation that preservation of cervical enamel and modification of palatal geometry may reduce localized tensile and shear stresses at the adhesive interface. However, these computational findings should be interpreted as supportive approximations rather than direct clinical validation [30, 31] [32, 33].

When these findings are situated within the broader literature on partial-coverage restorations, a coherent narrative emerges. Vertical or no margin protocols such as the biologically oriented preparation technique in monolithic zirconia have reported marginal gaps in the 50 µm range and fatigue survival above 85%, values closely tracking the performance of the MS design [34, 35]. Partial coverage onlays and vonlays fabricated from high-strength lithium disilicate similarly benefit from enamel level bonding and exhibit repair friendly fracture patterns [4]. The present study extends those observations by showing that deliberate axial reduction of only 0.4 mm, combined with a coronally displaced palatal finish, yields mechanical benefits that match or exceed those achieved by more aggressive circumferential design, without compromising aesthetics or retention.

The clinical ramifications of these results are multifaceted. A preparation that preserves cervical enamel simplifies adhesive protocols by permitting selective etching and reduces the need for aggressive isolation techniques [36]. By positioning the margin well clear of the sulcus, the design also facilitates cement removal and

Fig. 17 failure: catastrophic palatal root fracture extending

Fig. 18 Grade I fracture of MS preparation design

Table 6 FEA metrics by preparation design

Metric	MS	CF	Reduction
Peak von Mises at palatal cervical (MPa)	250	415	–40%
Max principal tensile stress in dentine (MPa)	41	71	–42%
Cement interfacial shear > 25 MPa (% nodes)	12%	29%	–59%
Crown tip displacement (µm) under 250 N	9.1	11.8	–23%

minimizes postoperative periodontal inflammation, a concern frequently voiced with CF design [16, 37]. From a conservative dentistry perspective, the predominance of restorable failure patterns observed in the MS group may support repair-oriented management strategies; however, any cost-related or sustainability-related benefits remain hypothetical and require direct clinical and life-cycle evaluation.

Several methodological limitations, however, temper the extrapolation of the current data to daily practice. Therefore, the findings should be interpreted as controlled preclinical evidence of thermo-mechanical behavior rather than direct proof of long-term clinical superiority. The in vitro model cannot replicate the enzymatic degradation of resin cement or the pH fluctuations of the oral environment, nor does it incorporate lateral

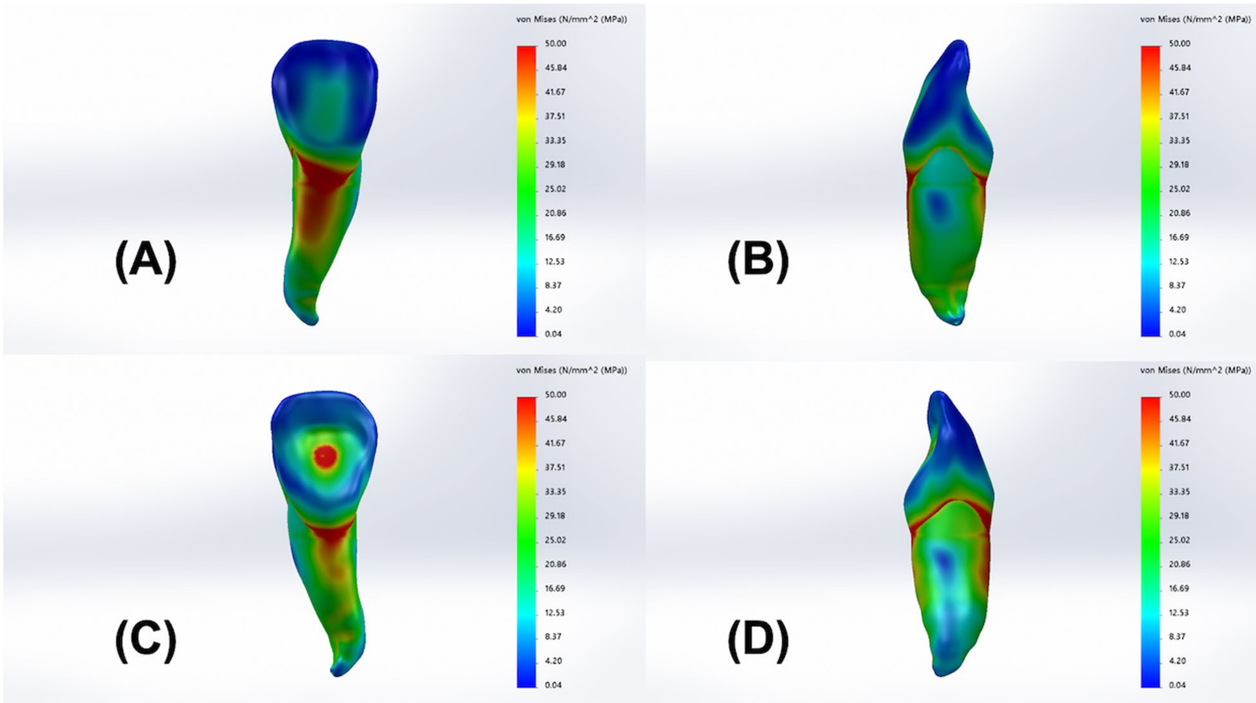

Fig. 19 Finite-element von Mises stress distribution in the conventional full-coverage (CF) model under a 250 N oblique palatal load applied at 45°. The color scale represents stress values in MPa. High stress concentration is observed at the palatal-cervical region of the zirconia crown

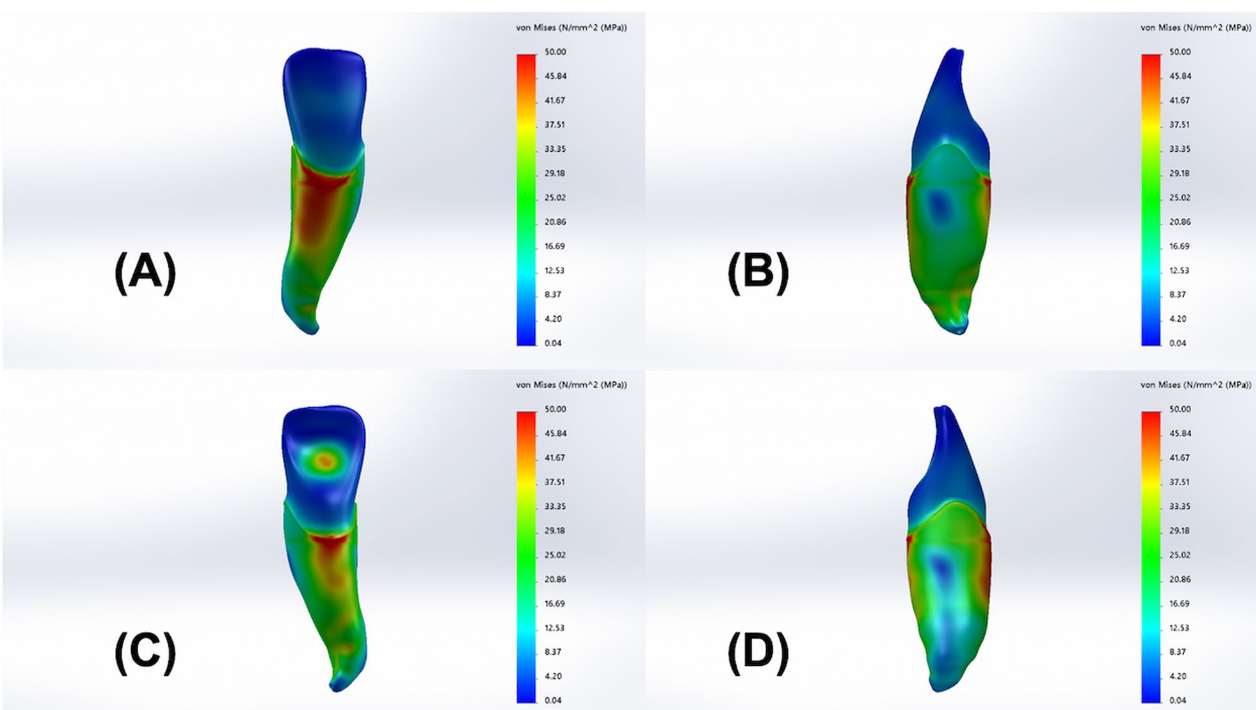

Fig. 20 Finite-element von Mises stress distribution in the prepared tooth and root of the conventional full-coverage (CF) model under a 250 N oblique palatal load applied at 45°. The color scale represents stress values in MPa. Higher stress concentration is observed in the palatal-cervical region and root area

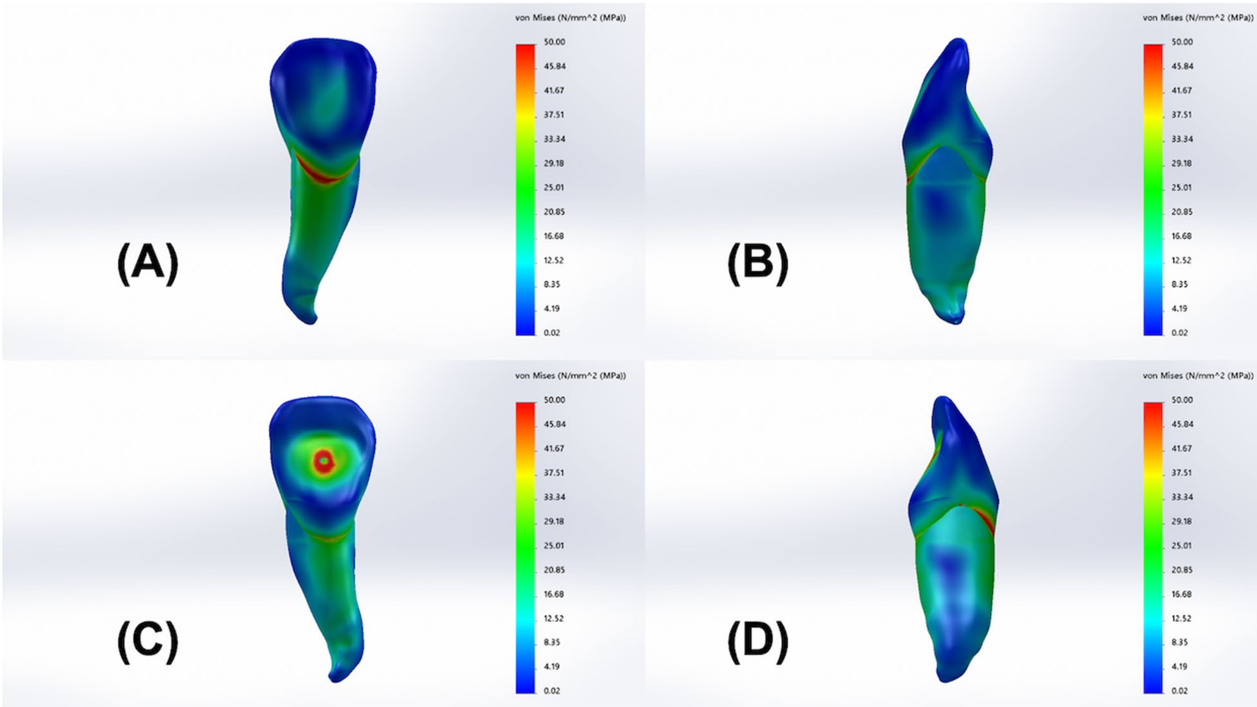

Fig. 21 Finite-element von Mises stress distribution in the Mini-skirt (MS) model under a 250 N oblique palatal load applied at 45°. The color scale represents stress values in MPa. Compared with the CF model, the MS design shows reduced palatal-cervical stress and a broader, more coronally distributed load-sharing pattern

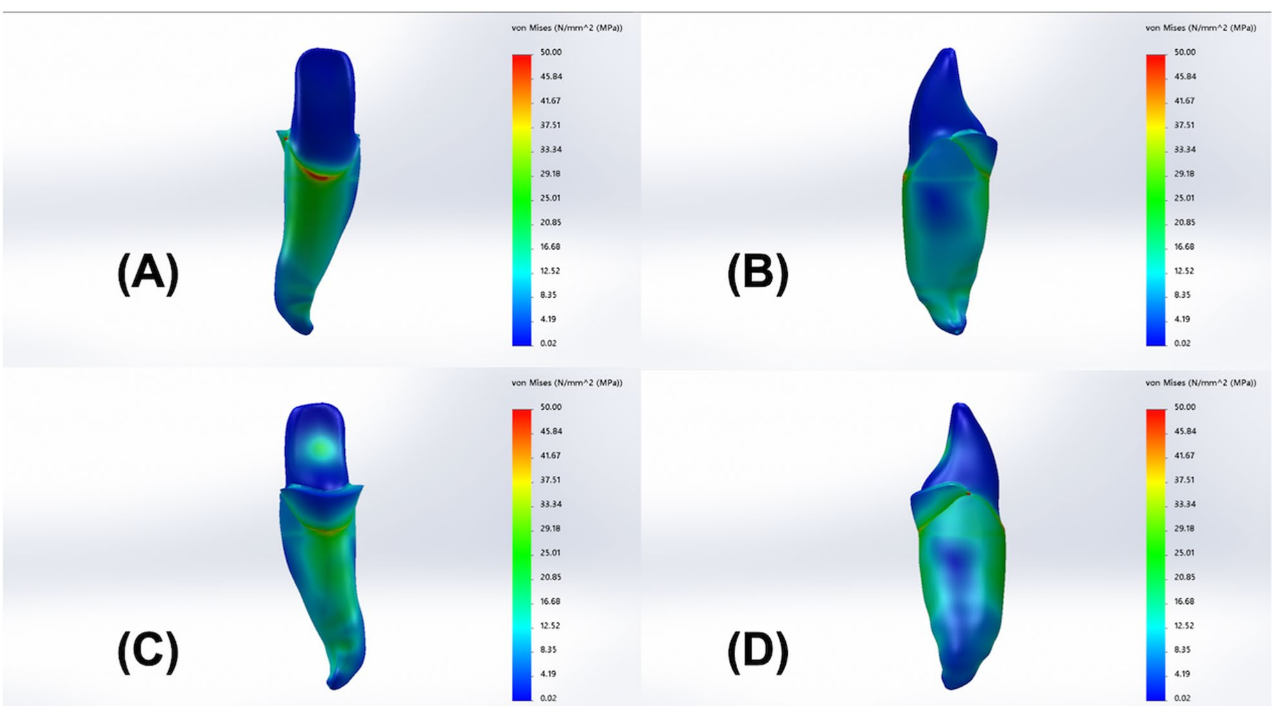

Fig. 22 Finite-element von Mises stress distribution in the prepared tooth and root of the Mini-skirt (MS) model under a 250 N oblique palatal load applied at 45°. The color scale represents stress values in MPa. Compared with the CF model, the MS preparation shows reduced palatal-cervical stress and a broader coronal stress distribution

Table 7 Summary of outcomes (MS vs. CF)

Outcome metric	Mini-skirt (MS)	Full-coverage (CF)	% Improvement	Statistical note
Fatigue run-outs ($n = 30$)	28/30 (93.3%)	16/30 (53.3%)	+40%	χ^2, $p < 0.01$
Risk ratio for failure	0.14	1 (ref.)	—	95% CI 0.04–0.58
Median fracture load (N)	1 140	860	+32%	Mann-Whitney
Mean marginal gap (μm)	67 ± 14	112 ± 21	−40%	Two-way ANOVA, $p < 0.001$
Restorable failures	83%	37%	+118%	χ^2, $p < 0.001$
Peak von Mises (MPa)	250	415	−40%	FEA

or protrusive functional patterns that may impose different stress vectors on anterior teeth [38, 39]. The use of 4Y zirconia limits direct inference to higher translucency but lower strength multi-layered systems, while the single-tooth model does not capture the splinting effects occasionally employed in clinical full-arch rehabilitations. Finally, although 1.7 million loading cycles represent an accepted surrogate for early clinical service, long-term trials beyond the decade mark remain essential to verify that the early mechanical and biological advantages translate into sustained superiority. In addition, the in vitro design cannot fully replicate the biological and functional complexity of the oral environment, including saliva, thermal variation over longer periods, patient-specific occlusal habits, masticatory variability, and periodontal/adaptive tissue responses. Therefore, the findings should be interpreted as controlled preclinical evidence of thermo-mechanical behavior rather than direct proof of long-term clinical superiority.

Future work should therefore expand the conservative-margin paradigm to newer translucent zirconia with reduced flexural strength, and to hybrid ceramics whose fracture modes differ from dense zirconia. In vivo studies tracking periodontal indices, marginal staining, and patient-reported outcomes will complement the purely mechanical data and provide a holistic appraisal of the technique's merits. Parametric finite-element studies varying skirt height and thickness could establish a design envelope that balances rigidity with masking capacity, and novel bio-adhesive cements with lower elastic modulus deserve exploration as they may further attenuate interface shear.

In summary, the combined findings from mechanical testing, marginal analysis, failure-mode profiling and finite-element simulation consistently favors the MS preparation, revealing higher fatigue survival, greater residual strength, tighter margins and a far more reparable fracture pattern than its CF counterpart. These findings validate the mechanistic premise that preserving cervical enamel and displacing the palatal finish line coronally redistributes stress away from the vulnerable cervical collar and moderates interfacial shear. Within the methodological limits of this in vitro model, the findings support the working hypothesis that the conservative MS design provides favorable thermo-mechanical performance compared with conventional CF preparations for generation-5 zirconia crowns.

Conclusions

Within the limitations of this in vitro study, the following could be concluded:

- The conservative Mini-skirt (MS) preparation demonstrated favorable biomechanical behavior compared with the conventional full-coverage (CF) preparation for anterior zirconia crowns under simulated thermo-mechanical loading.
- Preserving cervical enamel and relocating the palatal finish line appeared to improve stress distribution, marginal integrity, and failure-mode restorability within the tested laboratory conditions.
- Although these findings provide a biomechanical rationale for the MS design, long-term clinical studies are still required before routine clinical adoption can be recommended.

Abbreviations

MS	Mini-skirt
CF	Conventional full-coverage
FEA	Finite-element analysis
CEJ	Cementoenamel junction
SD	Standard deviation
IQR	Interquartile range
RR	Risk ratio

Acknowledgements
Not applicable.

Authors' contributions
MR, MS, and RE conceptualized and designed the study, coordinated the project, supervised data acquisition, contributed substantially to data interpretation, and drafted the manuscript. RT, DT, DE, and RE contributed to study design, data collection, and critical review of the manuscript. MB, OB, OM, and AN contributed to data acquisition, data curation, and manuscript editing. NS, SM, MM, HI, and MF contributed to data interpretation, methodological input, and critical revision for important intellectual content. MR and MS performed the final revision of the manuscript. All authors read and approved the final manuscript and agree to be accountable for all aspects of the work.

Funding
Open access funding will be covered by the Science, Technology & Innovation Funding Authority (STDF) in cooperation with the Egyptian Knowledge Bank (EKB). No additional funding was received for the study design; data collection, analysis, and interpretation; or manuscript writing.

Data availability
The datasets used and/or analyzed during the current study are available from the corresponding author on reasonable request.

Declarations

Ethics approval and consent to participate
Ethical approval was obtained from the Institutional Review Board, Faculty of Oral and Dental Medicine, Nahda University, Egypt (IRB No. 003-9-25-2). Extracted maxillary central incisors were obtained after informed patient consent, and all specimens were anonymized and coded. All methods were performed in accordance with IRB requirements and applicable institutional and national guidelines, and in compliance with the Declaration of Helsinki.

Consent for publication
Not applicable.

Competing interests
The authors declare no competing interests.

Author details
[1]Department of Fixed Prosthodontics, Faculty of Oral and Dental Medicine, Misr university for science and technology, Giza, Egypt
[2]Magrabi health, Magrabi hospital, King Fahed Road, Al Mohamadiah, Riyadh, Saudi ArabiaKSA
[3]Department of Prosthodontics, Dr. Sulaiman Al-Habib Medical Group, Riyadh, KSA, Saudi Arabia
[4]Department of Fixed Prosthodontics, Faculty of dentistry, Modern University for Technology & Information, Cairo, Egypt
[5]Department of Fixed Prosthodontics, Faculty of oral and dental medicine, Nahda University, Beni Suef, Egypt
[6]Department of Fixed Prosthodontics, Faculty of Dentistry, British University, Cairo, Egypt
[7]Department of Conservative and Restorative Dentistry, Nahda University, Beni Suef, Egypt
[8]Department of Fixed Prosthodontics, Faculty of Dentistry, MSA University, Giza, Egypt
[9]Department of Restorative and Prosthetic Dental Sciences, Dar Al Uloom University, Riyadh, Saudi Arabia
[10]Department of Fixed Prosthodontics, Faculty of Dentistry, Ahram Canadian university, Giza, Egypt
[11]Department of Prosthodontics, Faculty of Dentistry, Misr University for Science and Technology, Giza, Egypt
[12]Fixed Prosthodontics Department, Faculty of Dentistry, Minia University, Minia, Egypt
[13]Department of Dental Biomaterials, College of Oral and Dental Surgery, Misr University for Science and Technology (MUST), Giza, Egypt
[14]Department of Fixed Prosthodontics, Faculty of Dentistry, University, Galala Plateau, Attaka, Suez, Egypt

Received: 7 February 2026 / Accepted: 15 July 2026

References

1. Charoenporn W, Sornsuwan T, Sae-Lee D, Amornvit P, Chaijareenont P, Rungsiyakull P. Evaluating fatigue resistance in occlusal veneers: a comparative study of processing techniques and material thickness of lithium disilicate (IPS e.max Press vs. IPS e.max CAD). BMC Oral Health. 2024;24(1):1542. https://doi.org/10.1186/s12903-024-05347-7.
2. Yilmaz K, Aydin H, Özdemir E. Effects of a modified margin design, material, and loading type on the stress distribution of endocrowns: A 3D finite element analysis. Dent Mater J. 2025;44(4):435–45. https://doi.org/10.4012/dmj.2024-316.
3. Goodacre CJ, Campagni WV, Aquilino SA. Tooth preparations for complete crowns: an art form based on scientific principles. J Prosthet Dent. 2001;85(4):363–76. https://doi.org/10.1067/mpr.2001.114685.
4. Prott LS, Pieralli S, Klein P, et al. Survival and Complications of Partial Coverage Restorations on Posterior Teeth-A Systematic Review and Meta-Analysis. J Esthet Restor Dent. 2025;37(3):620–41. https://doi.org/10.1111/jerd.13353.
5. Alaida WS, Gadi SA, Al-Ghannam RE, et al. Biomechanical and Occlusal Factors Influencing the Longevity of Single-Unit Restorations: A Comprehensive Review. Cureus. 2025;17(6):e85998. https://doi.org/10.7759/cureus.85998.
6. Yamakami SA, Sehgal S, Taylor RH, Ohyama H. Decision tree protocol for demineralized gingival margin extension in class II composite cavity preparations. J Dent Sci. 2021;16(3):1050–3. https://doi.org/10.1016/j.jds.2021.01.016.
7. An H, Mickesh GJ, Cho D, Sorensen JA. Effect of finish line location and saliva contamination on the accuracy of crown finish line scanning. J Prosthodont. 2024;33(1):86–94. https://doi.org/10.1111/jopr.13658.
8. Alahmad AM, Alenezi AY, Rayyan M, et al. Static Loading of Different Intraradicular Preparation Depths of Trinia Endocrowns in Maxillary Canines. J Contemp Dent Pract. 2024;25(6):575–80. https://doi.org/10.5005/jp-journals-10024-3714.
9. Rayyan MM, Aboushelib M, Sayed NM, Ibrahim A, Jimbo R. Comparison of interim restorations fabricated by CAD/CAM with those fabricated manually. J Prosthet Dent. 2015;114(3):414–9. https://doi.org/10.1016/j.prosdent.2015.03.007.
10. Perdigão J. Current perspectives on dental adhesion: (1) Dentin adhesion - not there yet. Jpn Dent Sci Rev. 2020;56(1):190–207. https://doi.org/10.1016/j.jdsr.2020.08.004.
11. Paphangkorakit J, Leelayuwat N, Boonyawat N, Parniangtong A, Sripratoom J. Effect of chewing speed on energy expenditure in healthy subjects. Acta Odontol Scand. 2014;72(6):424–7. https://doi.org/10.3109/00016357.2013.847490.
12. Heintze SD, Eser A, Monreal D, Rousson V. Using a chewing simulator for fatigue testing of metal ceramic crowns. J Mech Behav Biomed Mater. 2017;65:770–80. https://doi.org/10.1016/j.jmbbm.2016.09.002.
13. Malysa A, Wezgowiec J, Grzebieluch W, Danel DP, Wieckiewicz M. Effect of Thermocycling on the Bond Strength of Self-Adhesive Resin Cements Used for Luting CAD/CAM Ceramics to Human Dentin. Int J Mol Sci. 2022;23(2):745. https://doi.org/10.3390/ijms23020745.
14. Bramanti E, Cervino G, Lauritano F, et al. FEM and Von Mises Analysis on Prosthetic Crowns Structural Elements: Evaluation of Different Applied Materials. ScientificWorldJournal. 2017;2017:1029574. https://doi.org/10.1155/2017/1029574.
15. Ayash GM, Ossman E, Segaan LG, Rayyan M, Joukhadar C. Influence of core color on final shade reproduction of zirconia crown in single central incisor situation - An in vivo study. J Clin Exp Dent. 2020;12(1):e46–51. https://doi.org/10.4317/medoral.56401.
16. Reslan MR, Sayed M, Rayyan MM, Farouk H. Effect of Cement Type on Fracture Resistance and Mode of Failure of Monolith vs Bilayered Zirconia Single Crowns. J Contemp Dent Pract. 2023;24(8):576–81. https://doi.org/10.5005/jp-journals-10024-3546.
17. Dghaily D, Rayyan M, Ragab H, Sayed M, Ayash G, Alzahrani G. Comparison of Fracture Resistance between Different Treatment Modalities of Mutilated Endodontically Treated Teeth Using Polyether Ether Ketone. J Contemp Dent Pract. 2023;24(9):668–73. https://doi.org/10.5005/jp-journals-10024-3558.
18. Sayed M, Alahmad AM, Alhajji KS, et al. Removal Efficiency and Effectiveness of Four Different Fiber Posts Using Five Different Drill Systems in Multirooted Teeth. J Contemp Dent Pract. 2024;25(1):72–8. https://doi.org/10.5005/jp-journals-10024-3629.
19. Pashley EL, Tao L, Pashley DH. Sterilization of human teeth: its effect on permeability and bond strength. Am J Dent. 1993;6(4):189–91.
20. Gaafar SS, El Mekkawi ARO, Farag RA, et al. Comparative analysis of the inflammatory response of human gingival fibroblasts to NeoSEALER Flo and CeraSeal bioceramic sealers: an in vitro study. BMC Oral Health. 2025;25(1):395. https://doi.org/10.1186/s12903-025-05692-1.
21. Gaafar SS, El Ballouli D, Rayyan M, Sayed M, Basta DG, Fouad M. Fracture resistance, failure mode and restorability of CAD CAM Zirconia endocrowns with different pulpal extension depths bonded to maxillary molars: an in-vitro study. BMC Oral Health. 2025;25(1):176. https://doi.org/10.1186/s12903-025-05466-9.
22. Ayash G, Osman E, Segaan L, Rayyan M, Joukhadar C. Influence of resin cement shade on the color and translucency of zirconia crowns. J Clin Exp Dent. 2020;12(3):e257–63. https://doi.org/10.4317/jced.56425.
23. Kongkiatkamon S, Peampring C. Comparison of Regular and Speed Sintering on Low-Temperature Degradation and Fatigue Resistance of Translucent Zirconia Crowns for Implants: An In Vitro Study. J Funct Biomater. 2022;13(4):281. https://doi.org/10.3390/jfb13040281.
24. Lundgren D, Laurell L. Occlusal force pattern during chewing and biting in dentitions restored with fixed bridges of cross-arch extension. II. Unilateral

posterior two-unit cantilevers. J Oral Rehabil. 1986;13(2):191–203. https://doi.org/10.1111/j.1365-2842.1986.tb00651.x.
25. Heydecke G, Butz F, Hussein A, Strub JR. Fracture strength after dynamic loading of endodontically treated teeth restored with different post-and-core systems. J Prosthet Dent. 2002;87(4):438–45. https://doi.org/10.1067/mpr.2002.123849.
26. Lundgren D, Laurell L. Occlusal force pattern during chewing and biting in dentitions restored with fixed bridges of cross-arch extension. I. Bilateral end abutments. J Oral Rehabil. 1986;13(1):57–71. https://doi.org/10.1111/j.1365-2842.1986.tb01556.x.
27. Partiyan A, Osman E, Rayyan MM, Aboushelib M, Ibrahim A, Jimbo R. Fracture resistance of three-unit zirconia fixed partial denture with modified framework. Odontology. 2017;105(1):62–7. https://doi.org/10.1007/s10266-016-0242-9.
28. Shihabi S, Chrcanovic BR. Clinical outcomes of tooth-supported monolithic zirconia vs. porcelain-veneered zirconia fixed dental prosthesis, with an additional focus on the cement type: a systematic review and meta-analysis. Clin Oral Investig. 2023;27(10):5755–69. https://doi.org/10.1007/s00784-023-05219-4.
29. Sailer I, Strasding M, Valente NA, Zwahlen M, Liu S, Pjetursson BE. A systematic review of the survival and complication rates of zirconia-ceramic and metal-ceramic multiple-unit fixed dental prostheses. Clin Oral Implants Res. 2018;29(Suppl 16):184–98. https://doi.org/10.1111/clr.13277.
30. Sakrana AA. In vitro evaluation of the marginal and internal discrepancies of different esthetic restorations. J Appl Oral Sci. 2013;21(6):575–80. https://doi.org/10.1590/1679-775720130064.
31. Rayyan MR. Marginal Adaptation of Monolithic High-Translucency Versus Porcelain-Veneered Zirconia Crowns. Int J Prosthodont. 2019;32(4):364–6. https://doi.org/10.11607/ijp.5985.
32. Talmazov G, Veilleux N, Abdulmajeed A, Bencharit S. Finite element analysis of a one-piece zirconia implant in anterior single tooth implant applications. PLoS ONE. 2020;15(2):e0229360. https://doi.org/10.1371/journal.pone.0229360.
33. Tsumanuma KTS, Caldas RA, Silva ID, Miranda ME, Brandt WC, Vitti RP. Finite Element Analysis of Stress in Anterior Prosthetic Rehabilitation with Zirconia Implants with and without Cantilever. Eur J Dent. 2021;15(4):669–74. https://doi.org/10.1055/s-0041-1727544.
34. Abad-Coronel C, Villacís Manosalvas J, Palacio Sarmiento C, Esquivel J, Loi I, Pradíes G. Clinical outcomes of the biologically oriented preparation technique (BOPT) in fixed dental prostheses: A systematic review. J Prosthet Dent. 2024;132(3):502–8. https://doi.org/10.1016/j.prosdent.2022.07.010.
35. Ayash G, Rayyan MM, Segaan L, Sayed M. In vivo Evaluation of Shade Replication of Different Generations of Zirconia to Natural Teeth Using Digital Color Determinations. J Contemp Dent Pract. 2023;24(8):545–50. https://doi.org/10.5005/jp-journals-10024-3554.
36. Josic U, Mazzitelli C, Maravic T, et al. The influence of selective enamel etch and self-etch mode of universal adhesives' application on clinical behavior of composite restorations placed on non-carious cervical lesions: A systematic review and meta-analysis. Dent Mater. 2022;38(3):472–88. https://doi.org/10.1016/j.dental.2022.01.002.
37. Chee WW, Duncan J, Afshar M, Moshaverinia A. Evaluation of the amount of excess cement around the margins of cement-retained dental implant restorations: the effect of the cement application method. J Prosthet Dent. 2013;109(4):216–21. https://doi.org/10.1016/S0022-3913(13)60047-5.
38. Rigos AE, Sarafidou K, Kontonasaki E. Zirconia bond strength durability following artificial aging: A systematic review and meta-analysis of in vitro studies. Jpn Dent Sci Rev. 2023;59:138–59. https://doi.org/10.1016/j.jdsr.2023.04.002.
39. Lughi V, Sergo V. Low temperature degradation -aging- of zirconia: A critical review of the relevant aspects in dentistry. Dent Mater. 2010;26(8):807–20. https://doi.org/10.1016/j.dental.2010.04.006.

Publisher's Note

Springer Nature remains neutral with regard to jurisdictional claims in published maps and institutional affiliations.